Use of Multidimensional Fluorescence Resonance Energy Transfer To Establish the Orientation of Cholecystokinin Docked at the Type A Cholecystokinin Receptor[†]

Kaleeckal G. Harikumar, Fan Gao, Delia I. Pinon, and Laurence J. Miller*

Department of Molecular Pharmacology and Experimental Therapeutics, Mayo Clinic, 13400 East Shea Boulevard, Scottsdale, Arizona 85259

Received April 24, 2008; Revised Manuscript Received July 21, 2008

ABSTRACT: Fluorescence resonance energy transfer (FRET) represents a powerful tool to establish relative distances between donor and acceptor fluorophores. By utilizing several donors situated in distinct positions within a docked full agonist ligand and several acceptors distributed at distinct sites within its receptor, multiple interdependent dimensions can be determined. These can provide a unique method to establish or confirm three-dimensional structure of the molecular complex. In this work, we have utilized full agonist analogues of cholecystokinin (CCK) with Aladan distributed throughout the pharmacophore in positions 24, 29, and 33, along with receptor constructs derivatized with Alexa^{546} at positions 94, 102, 204, and 341 in the helical bundle and first, second, and third extracellular loops, respectively. These provided 12 FRET distances to overlay on working models of the CCK-occupied receptor. These established that the carboxyl terminus of CCK resides at the external surface of the lipid bilayer, adjacent to the receptor amino-terminal tail, rather than being inserted into the helical bundle. They also provide important experimentally derived constraints for understanding spatial relationships between the docked ligand and the flexible extracellular loop regions. Multidimensional FRET provides a new independent method to establish and refine structural insights into ligand−receptor complexes.

INTRODUCTION

Understanding of the molecular basis of agonist docking with and activation of a receptor provides important insights into the conformation of this complex in the active state. Such molecular insights become extremely useful in the ligand-guided rational development and refinement of receptor-active drugs. For the superfamily of guanine nucleotide-binding protein (G protein)-coupled receptors (GPCRs) that represent the largest group of physiologically important cell surface receptors as well as the largest group of extant drug targets, we have little high resolution structural detail on which to rely. Until recently, rhodopsin represented the only member of this superfamily with a high resolution structure that had been solved (*1, 2*). Now, we also have structures for the β2-adrenergic receptor (*3, 4*). While the helical bundles for both have many similarities, the loop regions are very different. For the other members of this superfamily, current structural insights have come from homology modeling with the rhodopsin structure, with insights into mechanisms of docking coming from a variety of techniques, such as receptor mutagenesis, ligand structure−activity relationships, complementary two-dimensional mutagenesis, chimeric receptor characterization, photoaffinity labeling, and physicochemical analysis of isolated portions of receptors or receptor fragments (*5, 6*). Such diverse approaches can often yield contradictory results, requiring further experimental evaluation. Independent approaches can provide new insights capable of refuting specific aspects of a model, with the possibility of refining it.

The cholecystokinin (CCK)[1]receptor is a member of the rhodopsin family (Family A) of GPCRs that binds and is activated by a small peptide hormone secreted from I cells scattered throughout the proximal small intestine in response to protein and fat ingestion (*7−9*). The type A (also known as the type 1) CCK receptor is important for nutritional homeostasis, playing a role in postcibal stimulation of gallbladder contraction, exocrine pancreatic secretion, gastric emptying, enteric transit, and even satiety. Our current understanding of the molecular basis of CCK binding to this receptor has come from the types of studies listed above (*7, 9*). Despite extensive series of studies, two distinct molecular models continue to be proposed for the occupation of the CCK receptor with its natural hormonal peptide (*10, 11*). One of these molecular models has been developed predominantly based on photoaffinity labeling, utilizing intrinsic probes with sites of covalent attachment that are distributed throughout the pharmacophoric domain of the ligand (*10, 12−14*). The contrasting model has been developed based predominantly on the loss of function observed in response to receptor mutagenesis, as well as the functional impact of complementary modifications of the receptor and ligand residues proposed to interact with each other (*11, 15, 16*). It is not yet clear whether the recently released structures of the β2-adrenergic receptor will provide a more relevant and

[†] This work was supported by the National Institutes of Health Grant DK32878 (L.J.M.) and by the Fiterman Foundation.

* To whom correspondence should be addressed. Tel.: (480) 301-6650. Fax: (480) 301-6969. E-mail: miller@mayo.edu.

[1] The abbreviations used are the following: CCK, cholecystokinin; CHO, Chinese hamster ovary; FRET, fluorescence resonance energy transfer; KRH, Krebs-Ringers-HEPES medium.

10.1021/bi800734w CCC: $40.75
Published on Web 08/13/2008

improved template over rhodopsin that has been utilized in previous modeling.

Of note, while these two models of the CCK receptor bear a high degree of similarity in the proposed structure of the receptor, and even in the positioning of the amino terminus of the docked natural peptide ligand within that structure, the carboxyl terminus of CCK resides in quite distinct positions in the two models. In one model, the carboxyl terminus of CCK is proposed to reside adjacent to the receptor amino-terminal tail above transmembrane segment one (*13*), while, in the other model, it is proposed to reside within the intramembranous helical bundle (*17, 18*). Thus, the peptide is in a conformation that is folded back on itself in the first molecular model and elongated and linear in the second molecular model. Application of multidimensional fluorescence resonance energy transfer (FRET) to establish the relative distances (*19*) from various points in the docked CCK ligand to various points within the CCK receptor provides an opportunity to independently evaluate the predictions of these two models, and to potentially distinguish between them.

Precedent for this experimental approach was previously established (*20*−*22*). All of the controls to validate this approach in the current work were carefully performed. It is critical to note that each of the ligands utilized represents an analogue of the natural peptide hormone that has full agonist activity, and that each of the receptor variants utilized was capable of binding CCK normally and responding to CCK with a full biological response. We now apply FRET analysis to this experimental system to generate multiple dimensions between three points within CCK as docked at its receptor and four points within diverse extracellular regions of this receptor. These seem to discriminate between the proposed models, while providing important experimentally derived constraints for modeling the extracellular loops of this receptor.

EXPERIMENTAL PROCEDURES

Materials. Synthetic CCK-8 (representing residues 26 through 33 of CCK-33, the molecular form of this hormone that was first isolated and characterized) was purchased from Peninsula Laboratories (Belmont, CA); 2-aminoethylmethanethiosulfonate hydrochloride was from Toronto Research Chemicals (Ontario, Canada); Alexa^{546}-*N*-hydroxysuccinimide, Ham's F-12 culture medium, and antibiotic supplements were from Invitrogen (San Diego, CA); Fetal Clone II medium supplement was from Hyclone Laboratories (Logan, UT); and nonenzymatic cell dissociation solution was from Sigma-Aldrich (St. Louis, MO). All other reagents were analytical grade.

Preparation of Aladan Fluorescence Donors and Alexa^{546} Fluorescence Acceptors for FRET Studies. As fluorescence donors for our studies, we utilized three fluorescent CCK analogues that we previously prepared to incorporate Aladan (*N*-(diphenylmethylene)glycine tert-butylester) into distinct positions at the amino terminus, carboxyl terminus and midregion of the CCK pharmacophore (*23*). These CCK analogues were demonstrated to bind to the type A CCK receptor saturably and specifically with high affinity, and to represent full agonists, stimulating intracellular calcium responses similar to natural hormone. The steady-state fluorescence characteristics of these ligands while free in solution and while bound to the CCK receptor have previously been described (*23*).

Fluorescence acceptors for these studies were prepared by chemical derivatization of pseudowild type, monocysteine-reactive CCK receptor constructs stably expressed on Chinese hamster ovary (CHO) cell lines. These were previously prepared, characterized, and used in a more limited FRET study that measured only distances from the amino terminus of a CCK analogue (*22*). A thiol-reactive fluorescent Alexa-derivatization reagent (Alexa^{546}-MTS) was prepared by acylation of the free amino group of 2-aminoethylmethanethiosulfonate hydrochloride with Alexa^{546}-*N*-hydroxysuccinimide ester (*22*). This reagent was then utilized to derivatize single, accessible cysteine residues in the monoreactive CCK receptor constructs (*24*). This process yielded Alexa^{546}-labeled fluorescence acceptors in the receptor in position 94 (within the helical confluence, adjacent to transmembrane segment two), position 102 (first extracellular loop), position 204 (second extracellular loop), and position 341 (third extracellular loop). The fluorescence characteristics of Alexa are relatively insensitive to its environment, yielding similar excitation and emission characteristics that are independent of site of labeling this receptor.

Cell Culture and Receptor Derivatization. CHO cells stably expressing the various CCK receptor constructs were grown in tissue culture plastic dishes containing Ham's F-12 medium supplemented with 5% Fetal Clone II in a humidified chamber. Cells were passaged approximately twice per week.

Single reactive cysteine groups present within the ectodomain of the CCK receptor could be derivatized with the Alexa^{546}-MTS reagent, as we have described (*22*). This is a highly efficient reagent that was utilized in molar excess to ensure quantitative derivatization of accessible cysteine residues. For this procedure, cells were harvested using nonenzymatic cell dissociation medium, washed, and incubated with 1 μM cell-impermeant Alexa^{546}-MTS reagent for 20 min at room temperature in Krebs-Ringer-HEPES (KRH) medium containing 25 mM HEPES, pH 7.4, 104 mM NaCl, 5 mM KCl, 2 mM $CaCl_2$, 1 mM KH_2PO_4, and 1.2 mM $MgSO_4$. The unreacted MTS reagent was removed by repeated washing and centrifugation. Some control cells were not treated with the Alexa^{546}-MTS reagent, to provide donor-only conditions. The Alexa^{546}-labeled and control CCK receptor-bearing cells were then incubated with 100 nM Aladan-CCK ligands for 2 h at 4 °C. The fluorescently labeled cells were then washed with cold KRH medium and resuspended in cold medium in preparation for FRET studies.

Fluorescence Resonance Energy Transfer (FRET) Measurements. All steady-state fluorescence intensities were collected using the same Fluoromax-3 fluorometer (SPEX industries, Edison, NJ) at 25 °C with a quartz cuvette (1 cm path length). Fluorescence emission spectra were recorded in 1 nm increments from 430 to 650 nm after excitation at 362 nm. Excitation spectra were acquired by measuring emission intensity at 572 nm upon excitation with light at wavelengths ranging from 470 to 570 nm, and were reported as recorded fluorescence on the wavelength scale. Spectra collected under identical experimental conditions, using each of the Aladan-containing ligands with Alexa-derivatized preparations of nonreceptor-bearing untransfected cells, were

utilized to correct for background fluorescence and light scatter. This represented 2.2 to 2.7% of the fluorescence signal in the analogous experimental condition, resulting in a correction of FRET calculations that was consistently less than one percent of the ultimate distance determination. The corrected values were utilized for all calculations. It is noteworthy that the fluorescence characteristics of the donor (Aladan) varied with its position within the CCK analogues, while the fluorescence characteristics of the Alexa seemed to be unaffected by its position within the CCK receptor.

The Förster equation, $R_o = 9786(Jn^{-4}\kappa^2 Q_D)^{1/6}$ Å, is utilized to determine the distance between a fluorescence donor and acceptor at which 50% of the donor energy is transferred to the acceptor. This represents a special circumstance that is determined by the overlap integral calculated using the fluorescence emission spectrum of the donor-only condition (with no acceptor) and the absorption spectrum of the acceptor-only condition (with no donor). The other variables in this equation are the following. The refractive index for an aqueous medium ($n = 1.4$) was used, since the Aladan donor is attached to a soluble dissociable ligand that has been shown to reside above the lipid bilayer and the Alexa acceptor is also quite hydrophilic. Further, potassium iodide quenching experiments have demonstrated that each of these positions within CCK ligands bound to the CCK receptor are highly water-accessible (*23*). Q_D represents the fluorescence quantum yield of the donor in the absence of acceptor. Donor ligand (Aladan) quantum yields were determined based on the comparison of emission intensities with that of quinine sulfate in 1 N H_2SO_4.

The value of 2/3 was utilized to reflect the relative orientation of the transition dipole of donor and acceptor fluorophores (κ^2). This approximation is widely utilized in this type of study, and is considered to be valid as long as donor and/or acceptor exhibit isotropic, dynamic orientation within the time-scale relevant to the studies. In support of this, substantial rotational freedom of motion has been demonstrated for the donor fluorophores within these probes as they are bound to the CCK receptor. Time-resolved anisotropies of the probes bound to the CCK receptor were measured using time-correlated single photon counting (*25*). Receptor-bound probes were excited at 25 °C in a quartz cuvette (1 cm path length) with a pulse-picked, frequency-doubled titanium-sapphire picosecond laser source (Coherent Mira 900, Palo Alto, CA) using 6.8 nm bandwidth interference filters. The excitation wavelength was tunable with a pulse width of approximately 2 ps full-width half-maximum. Data were collected in 1080 channels, with a width of 10.05 ps/channel. Fluorescence intensity decay analysis was performed using the GLOBALS Unlimited program, evaluating both models of single exponential and dual discrete exponential lifetime components and determining the best fit based on Chi-squared analysis. Each of the receptor-bound probes displayed two significant discrete rotational correlation times (φ), believed to reflect segmental motions and overall protein rotation. These represented 4.5 ± 1.4 and 17 ± 3.1 ns for the Aladan 24 probe, 8.7 ± 1.0 and 26.6 ± 8.7 ns for the Aladan 29 probe, and 3.7 ± 0.3 and 19.9 ± 3.4 ns for the Aladan 33 probe. The faster components, representing segmental motions, are believed to be most important to randomize the orientation factor (κ^2). These were of similar magnitude (within a factor of 2) to the measured fluorescence lifetimes (3.3 ± 0.25, 3.8 ± 0.15, and 3.4 ± 0.22 ns, respectively). Consistent with these segmental motions and the accessibility of the donor fluorophores to the hydrophilic milieu, the receptor-bound probes exhibited steady-state anisotropy values of 0.13 ± 0.01, 0.09 ± 0.01, and 0.12 ± 0.01, respectively. These corresponded to polarization values of 0.18 ± 0.01, 0.11 ± 0.02, and 0.17 ± 0.01, respectively. The steady-state anisotropy of the fluorescence acceptor in this experimental system was 0.08 ± 0.01, corresponding to a polarization value of 0.11 ± 0.01. For donor and acceptor fluorophores with mixed polarization, having values less than 0.3, the potential error in calculated distances has been projected to be below 10% (*26*).

The same equation was applied to the experimental conditions for the FRET studies in which each of the Aladan-CCK ligands (donors) were utilized with each of the Alexa^{546}-CCK receptor constructs (acceptors). In these experiments, the observed summation spectra that included both donor and acceptor emission were deconvoluted to identify the component donor and acceptor emission spectra, matching the peak fluorescence of both to achieve optimal concurrence. The summation spectra were found to be within two percent of the sum of the component spectra, and this was quite consistent from condition to condition. The acceptor emission spectrum was then utilized to determine the acceptor excitation responsible to produce it. Alexa^{546} has quantum yield and emission spectrum that are independent of excitation wavelength (data not shown) (*27*), providing evidence for its absorption spectrum being essentially superimposable on its excitation spectrum. The excitation spectrum of the acceptor was, therefore, considered to represent its absorption spectrum, permitting the calculation of the acceptor extinction coefficient. The overlap integral (J) was calculated using the equation, $J = \int F(\lambda)\varepsilon(\lambda)\lambda^4\, d\lambda / \int F(\lambda)\, d\lambda$, where $F(\lambda)$ is the fluorescence intensity of the donor at wavelength λ and $\varepsilon(\lambda)$ is the extinction coefficient of the acceptor.

The distances determined in the application of this equation were then corrected to yield proximal distances between donor and acceptor, using the efficiencies of energy transfer (E). These were determined based on the equation, $E = 1 - F_{DA}/F_{D,}$ where F_{DA} represents fluorescence of the donor in the presence of acceptor, determined in cells expressing each of the monoreactive receptor cysteine residues that had been treated with Alexa-MTS, and F_D represents fluorescence of the donor in the absence of acceptor, determined in the same cells that had not been treated with the Alexa-MTS reagent. While the distance determined using the conditions applied to the classical Förster equation does not require correction, since energy transfer is by definition 0.5 (50%), those distances determined with the application of this equation to the conditions of the FRET experiments in which efficiencies of energy transfer may be different from 0.5 (50%) required correction using the equation, $R = R_o[(1 - E)/E]^{1/6}$ Å.

Molecular Modeling. Two contrasting molecular models for CCK docked to its receptor that are in the current literature were utilized to determine relevant distances (*10, 11*). The helical bundles of these models are similar, having both been influenced by the crystal structure of rhodopsin (*1*). Additionally, the extracellular loops have some similarities, with both docked ligand models shown to exhibit spatial

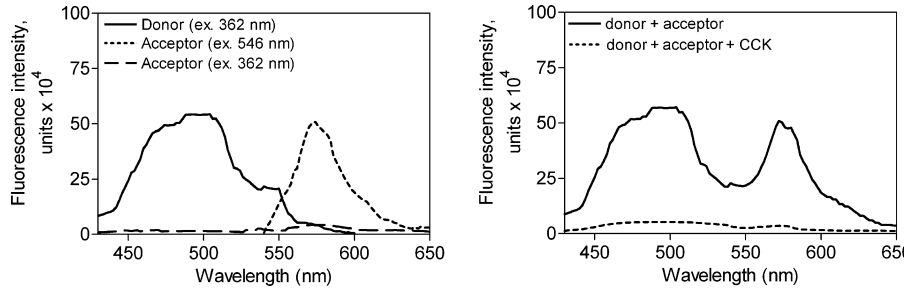

FIGURE 1: Control spectra. Shown are representative emission spectra of a fluorescence donor (Aladan[24]-CCK) bound to a monoreactive CCK receptor construct (N102C) after excitation with 362 nm light, and that of the same receptor derivatized with the fluorescence acceptor, Alexa[546], after excitation with light at either 362 nm or at 546 nm (left panel). This clearly establishes that the wavelength of light used to excite the donor has no ability to excite the acceptor in the absence of energy transfer from donor to acceptor. Also shown is the elimination of the FRET signal when nonfluorescent CCK (1 μM) competed for occupation of this monoreactive receptor by the fluorescence donor (right panel). This establishes the critical nature of spatial approximation between donor and acceptor provided by receptor occupation of donor in the experimental paradigm.

approximation between Arg[197] within the second loop and the sulfate moiety on the tyrosine residue in the 27 position of CCK (*10, 15, 28*). These models, however, exhibit major differences in the mode of docking of the remainder of CCK, with the carboxyl terminus demonstrated to be adjacent to the amino-terminal tail in the model based on photoaffinity labeling (*10*) and inserted into the helical bundle in the other model that is based largely on mutagenesis data (*11*). The differences in these models result in substantial differences in the predicted distances from residues within CCK and residues within the CCK receptor. Distances between the residues in the positions of the fluorescence donors within docked CCK and the receptor residues representing the positions of the fluorescence acceptors within the receptor were measured in the two models. These distances were compared with those measured in the current FRET studies, evaluating whether they were included within the 95% confidence intervals determined by the FRET analysis. Those distances from the models being evaluated that were outside of this confidence interval were identified.

RESULTS

This study took advantage of a validated approach to the in situ measurement of distances from a position within a CCK ligand and positions in the ectodomain of the CCK receptor. This was previously applied to a fluorescence donor at the amino terminus of CCK docked at special fluorescent CCK receptor constructs (*21, 22*). Subsequently, additional analogues of CCK with fluorescence reporters in the midregion and carboxyl terminus of the peptide having the appropriate characteristics to be utilized as FRET donors have been developed (*23*). These probes have the additional advantage of having the fluorescence donor, Aladan, incorporated as an amino acid variant directly into their peptide backbone. This provides the opportunity to now perform multidimensional FRET as these full agonist probes are normally docked at the CCK receptor. The ability to measure FRET distances from the carboxyl terminus of CCK turned out to be particularly important to distinguish between the currently proposed molecular models of the CCK-occupied receptor.

A series of experiments was critical to establish the validity of this strategy of utilizing the energy transfer between the fluorescence donor within the ligand and the fluorescence acceptor within the receptor to calculate meaningful distances. Both the ligands and the receptor constructs utilized in the studies must behave like natural full agonists and wild type receptor, as has been well established (*23*). The fluorescence characteristics of donor and acceptor are also important. Emission spectra from a representative pair of fluorescence donor and acceptor are illustrated in Figure 1. The fluorescence donor peptide exhibited its emission peak at 498 nm after excitation at 362 nm. The sample preparation including the CCK receptor that was tagged with fluorescence acceptor exhibited clear emission at 572 nm after excitation with light at 546 nm, with no significant emission in this region of the spectrum observed when the preparation was exposed to excitation with light at 362 nm. This demonstrated an acceptable level of specificity of the signal representing energy transfer between the donor and the relevant acceptor. Also shown is the fluorescence emission observed when nonfluorescent CCK is utilized to compete for the binding of Aladan-CCK to the receptor. When Aladan-CCK probes occupied the Alexa[546]-derivatized CCK receptor constructs, significant fluorescence energy transfer occurred with emission at 572 nm after excitation at 362 nm. A representative spectrum in this type of experiment that shows a clear FRET signal can be seen in Figure 2. A significant FRET signal was produced by each of the 12 pairs of ligand donor and acceptor-derivatized monoreactive CCK receptor in these studies.

A series of controls are critical for such studies. The measured energy transfer should occur only between the specified donor and acceptor. This was well established for the donors utilized in this work, given the high degree of specificity and high affinity of binding of the modified CCK ligands and the delivery of the fluorescence donor as an intrinsic part of these ligands. For the acceptors, there is a clear need for additional controls that demonstrate that nonreceptor membrane proteins that we know to be fluorescently labeled in the experimental system do not participate in meaningful energy transfer (*22*). Here, the advantage of performing the fluorescence labeling of the receptor in situ more than offsets the disadvantages of having the nonreceptor proteins labeled. In such a system, we can be confident that the receptor has normal polarity and insertion into the plasma membrane where it is fully biologically active. Control studies with nonreceptor-bearing cells, with receptor-bearing cells in the presence of excess competing nonfluorescent ligand, and with cells expressing null-cys-

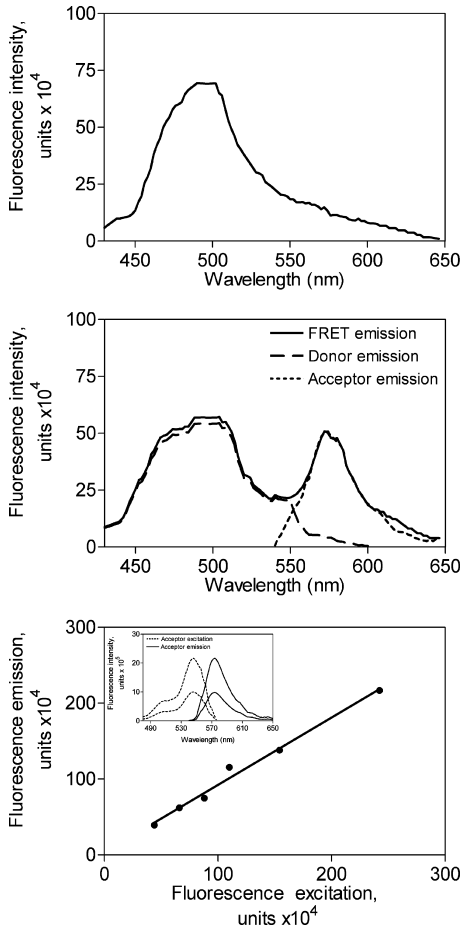

FIGURE 2: Experimental spectra. Shown are representative data generated with cells stably expressing the null-cysteine-reactive CCK receptor construct (top panel) and a representative pseudowild type, monocysteine-reactive CCK receptor construct (N102C) (middle panel). The cells were derivatized with the Alexa^{546}-MTS reagent and subsequently allowed to bind fluorescent Aladan ligand, as described in Methods. Cells were then excited by light at 362 nm and the illustrated emission spectra were collected. A peak at 572 nm in the monoreactive receptor-bearing cells indicates significant fluorescence resonance energy transfer, while the null-cysteine-reactive CCK receptor-bearing cells did not have such a peak. Also shown in the middle panel is the ability to deconvolute the FRET emission spectrum into its component donor emission and acceptor emission spectra. The bottom panel shows the calibration of Alexa fluorescence acceptor excitation and acceptor emission spectra, permitting the determination of the acceptor excitation associated with any observed acceptor emission. The Pearson correlation coefficient, "*r*", for the relationship between values of acceptor excitation and acceptor emission was 0.99.

teine-reactive receptor each yielded no significant FRET signal, despite having the nonreceptor membrane proteins labeled with acceptor (Figures 1 and 2). This established that the distances were too far between the receptor and other membrane proteins for meaningful energy transfer to occur.

The Förster distances calculated based on the spectra acquired in donor-only and acceptor-only experimental conditions were approximately 26 Å for each of the Aladan probes as donor and Alexa^{546} as acceptor. It was not clear that these conditions were fully applicable to each of the experimental conditions in which there was another structural modification of the receptor, with the introduction of the Alexa moiety into one of the ectodomains of the receptor. Therefore, the fluorescence emission spectra acquired in each of the specific experimental conditions for FRET were also

Table 1: (A) Spectral Overlap between Donors and Acceptors,[a] (B) Quantum Yields of Donor Probes Bound to the Noted Receptor Constructs, and (C) Efficiency of Energy Transfer between Donors and Acceptors[a]

site of receptor labeling	J × 10^{-15} cm^3 M^{-1}		
	Aladan^{24}-CCK	Aladan^{29}-CCK	Aladan^{33}-CCK
(A) Spectral Overlap between Donors and Acceptors			
C94	3.6 ± 1.0	4.2 ± 0.8	3.5 ± 1.2
N102C	0.9 ± 0.3	0.9 ± 0.1	1.2 ± 0.3
A204C	8.3 ± 3.9	3.3 ± 1.4	10.0 ± 3.1
T341C	0.7 ± 0.3	0.9 ± 0.4	0.6 ± 0.2
site of receptor labeling	Aladan^{24}-CCK	Aladan^{29}-CCK	Aladan^{33}-CCK
(B) Quantum Yields of Donor Probes Bound to the Noted Receptor Constructs			
C94	0.29	0.29	0.33
N102C	0.29	0.30	0.33
A204C	0.30	0.27	0.31
T341C	0.30	0.28	0.32
site of receptor labeling	%		
	Aladan^{24}-CCK	Aladan^{29}-CCK	Aladan^{33}-CCK
(C) Efficiency of Energy Transfer between Donors and Acceptors			
C94	56 ± 1.4	55 ± 1.1	58 ± 1.7
N102C	64 ± 2.3	66 ± 1.1	70 ± 3.5
A204C	53 ± 1.7	54 ± 2.3	53 ± 1.8
T341C	64 ± 1.8	67 ± 1.2	66 ± 1.5

[a] Values are expressed as means ± S.E.M. of data from a minimum of four to five independent experiments.

Table 2: Corrected Proximal Distances between Donors and Acceptors[a]

site of receptor labeling	Å		
	Aladan^{24}-CCK	Aladan^{29}-CCK	Aladan^{33}-CCK
C94	21.7 ± 1.0	22.7 ± 0.6	21.2 ± 1.2
N102C	16.5 ± 0.7	16.5 ± 0.3	15.9 ± 1.0
A204C	24.5 ± 2.5	21.0 ± 1.5	25.8 ± 2.5
T341C	15.9 ± 0.8	16.3 ± 0.4	15.8 ± 0.7

[a] Values are expressed as means ± S.E.M. of data from a minimum of four to five independent experiments.

analyzed directly. These summation emission spectra were divided into component emission spectra of Aladan donors and Alexa acceptors, with the latter used to determine the acceptor excitation spectrum that is superimposable on the acceptor absorption spectrum (Figure 2). This, in turn, was utilized in the calculation of the spectral overlap integral (Table 1A). The quantum yields of each of the donors bound to each of the monoreactive CCK receptor constructs used in this study were measured (Table 1B). These values and the constants described in the Methods were entered into the Förster equation, with the results corrected for efficiencies of energy transfer (Table 1C) to yield the proximal distances between donor and acceptor (Table 2).

This technique is most powerful to provide relative, rather than absolute, distances, since the assumptions utilized to populate the components of the equation can yield uncertainties that can be estimated to be as high as 11% in this type of experiment (*19, 29*). Of note, each of the three positions within CCK, at the amino terminus, midregion, and carboxyl terminus, was found to reside in a position that was a similar distance from the fluorescence acceptor situated high within the confluence of helices after derivatizing a cysteine residue in transmembrane segment two. Looking at the distances to

Table 3: Distances between Positions of Fluorescence Donors within CCK and Fluorescence Acceptors within the CCK Receptor in Two Contrasting Published Molecular Models[a]

	model 1 photoaffinity labeling (*10*)			model 2 receptor mutagenesis (*11*)		
	R, Å					
CCK position	24	29	33	25[b]	29	33
Receptor 94 position	24.0	22.8	21.0	26.9	19.6	12.9[c]
Receptor 102 position	14.2	12.8	16.2	17.3	15.4	16.8
Receptor 204 position	28.0	24.0	25.8	32.3	26.2	24.4
Receptor 341 position	13.4	14.2	15.7	20.0	14.9	19.0[c]

[a] Note: distances measured from C_β of the residue within CCK to the C_β of the corresponding receptor residue, except when the residue is a glycine, at which time C_α was utilized in the measurement. [b] There is no residue in position 24 in this model: therefore, the position 25 residue was utilized as an approximation for this measurement. [c] Marks distances outside of the 95% confidence interval that includes the distances determined in the FRET analysis.

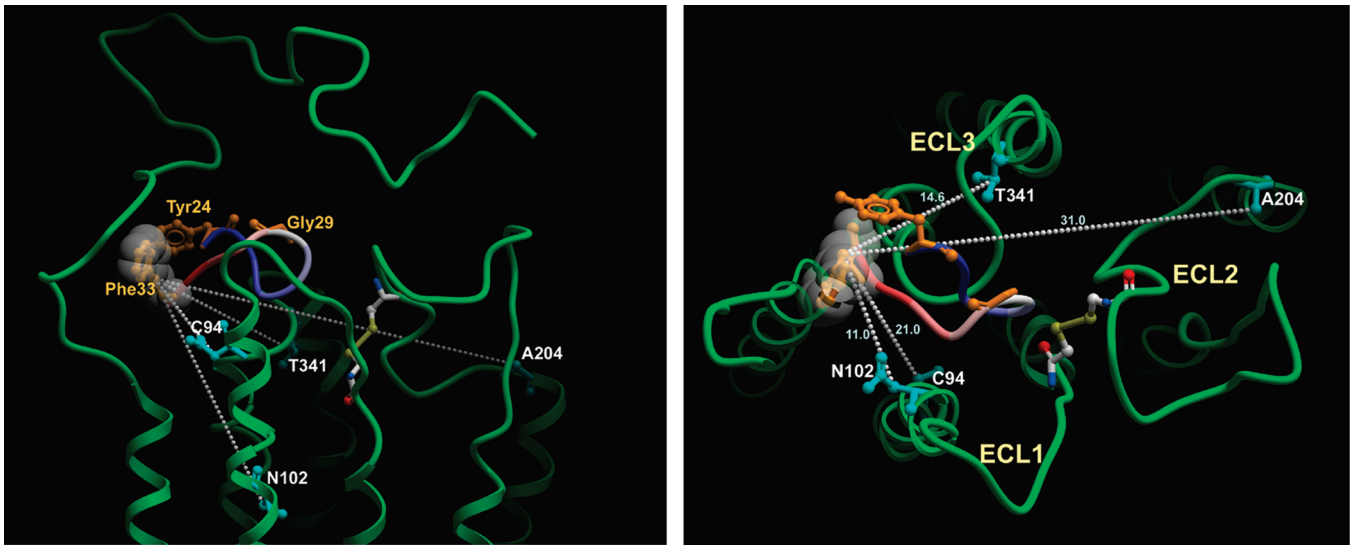

FIGURE 3: Molecular model of the CCK-occupied CCK receptor. Shown are views from the side (left panel) and top (right panel) of the molecular model of the CCK-occupied CCK receptor that is based on photoaffinity labeling data (*14*). This model is fully compatible with all twelve of the current experimentally derived FRET distance constraints. Highlighted in dashed white lines are the four distances between the C_β positions of the fluorescence donor at the critical residue at the carboxyl terminus of CCK (Phe^{33}) and the sites of the fluorescence acceptors within the CCK receptor. These distances best distinguish the two divergent working models of the CCK-occupied receptor, with the carboxyl terminus of the peptide situated in substantially different places in the two models. The backbone of the CCK ligand is illustrated in blue-to-red from amino terminus to carboxyl terminus. The sites of fluorescence donors are expanded and labeled. Each of the extracellular loop (ECL) regions of the CCK receptor is labeled. The disulfide bond that links extracellular loops one and two is illustrated as well.

each of the extracellular loops, each of the three ligand donors was most distant from residue 204 within the second loop. The shortest distances were those to the first and third loop regions.

Comparison of the distances measured using multidimensional FRET and those predicted by the two dominant molecular models of CCK-occupied receptor in the current literature is shown in Table 3. All of the measured distances in the FRET studies were compatible with the model based on photoaffinity labeling data (*10, 14*) In contrast, for the model based largely on receptor mutagenesis data (*11, 15, 16*), the measured distance between residue 33 of CCK (its carboxyl terminus) and Cys^{94} in the intramembranous helical bundle of the receptor was significantly shorter than the distance measured in the FRET studies. The other significant difference was the distance between residue 33 of CCK and Cys^{341}, being longer in this model than that measured in the FRET studies. Figure 3 illustrates the distances between the carboxyl-terminal residue in position 33 of CCK (key differentiator of the proposed models) and the positions of the fluorescence acceptors within the CCK receptor for the best model that is based on photoaffinity labeling data (*10*).

DISCUSSION

In the current absence of a crystal or NMR structure of a specific agonist-docked GPCR, many divergent and less definitive experimental approaches have been taken to gain insights into the conformation of the complex and into the molecular basis of ligand binding and activation. In the case of the CCK receptor, these approaches have yielded working models of the hormone-bound receptor that share many similarities, yet differ particularly in regard to the mode of docking the carboxyl-terminal portion of CCK (*10, 11*). In the current work, we have utilized multidimensional FRET to establish distances between residues scattered throughout the docked CCK ligand and residues in distinct extracellular regions of this receptor to try to gain new, independently derived insights, and to possibly distinguish between the molecular models that have been proposed. Multidimensional FRET becomes extremely powerful, considering that this approach in the current work, using three ligands and four receptor constructs, generates twelve distance constraints.

Both of the proposed models of CCK docked at its receptor share substantial similarities in their helical bundle domains

(*10, 11*). These structures are also quite similar to this region of the high resolution crystal structures of rhodopsin and the β2-adrenergic receptor (*1, 3*), consistent with the close primary structural relationships of the predicted transmembrane segments of those receptors with the CCK receptor. It is notable that the distances measured in the FRET studies from a residue fixed high in the intramembranous region of the central core of the helical bundle of the CCK receptor, at the level of Cys^{94} in transmembrane segment two, are not different to the amino terminus, midregion, and carboxyl terminus of CCK. These distances of approximately 22 Å are fully consistent with the peptide lying at the surface of the membrane, as has been proposed in the model based on photoaffinity labeling (*10, 14*). In contrast, this experimentally derived distance from the carboxyl terminus of CCK makes the model in which this region of CCK is proposed to reside immediately adjacent to Cys^{94} much less likely.

The microenvironment of the fluorophore at the carboxyl terminus of CCK as docked at its receptor was recently demonstrated to be exposed to hydrophilic solvent, based on potassium iodide quenching, and highly mobile, based on fluorescence anisotropy (*23*). Of particular note, the quenching of the carboxyl-terminal fluorescence indicator was even more pronounced when the receptor was in its active conformation than when in its inactive conformation (*23*). This is the opposite of what might be expected if activation involved moving the carboxyl terminus of CCK more deeply into the helical bundle. These fluorescence data are fully consistent with the current FRET data and with the molecular model derived from photoaffinity labeling data (*10*), again distinguishing it from the less-compatible model that places the peptide carboxyl terminus within the helical bundle (*11*).

The FRET distances to the extracellular loop regions are more difficult to interpret than those to the helical bundle region. This relates to the less well refined structures of the loops and the absence of experimentally generated constraints for those regions. In fact, the current FRET distances to the residues within each of these loops will represent important new constraints for building more meaningful models of the extracellular regions of this receptor. Evaluating compatibility of these distances with the existing models, it becomes clear that, while many of the distances measured are compatible with both proposed molecular models of the hormone-receptor complex, only the working model derived largely based on the photoaffinity labeling data (*10*) is fully compatible with all of the FRET distance constraints.

It is interesting that the FRET studies identified that the longest distances from all three of the CCK fluorophores to any of the extracellular loops were those to residue 204 within loop two. The second extracellular loop is the longest of the loops, constrained only by the presence of the architecturally important disulfide bond between the first and second loops that has been shown to be present in many GPCRs (*30*). That bond (involving Cys^{196}) is present nine residues away from residue 204. It is also interesting that the Arg^{197} residue adjacent to this disulfide bond has been proposed to interact with the sulfate moiety within tyrosine 27 of CCK in both working models (*10, 15*). This was determined using multiple different experimental approaches, including direct photoaffinity labeling. Here, too, this residue is eight residues away from residue 204 that was utilized as a site of one of the fluorescence acceptors in the current study. The long distance to this residue might suggest that part of the second extracellular loop might move away from the docked peptide.

The short distances to residues within the first and third extracellular loops is consistent with the peptide-binding pocket situated nestled between these loops. This is consistent with both models that have been proposed (*10, 11*), although detailed, experimentally based resolution of these loops has not yet been achieved.

The current report has utilized a unique and complementary technique to provide insights into the mode of docking the CCK natural peptide ligand to its Family A GPCR. The distance constraints are fully consistent with one of the models proposed in the current literature (*10*) and are less compatible with some features of the other model currently proposed (*11*). In addition to distinguishing between these models, the current data provide the first comprehensive set of experimentally derived constraints for the extracellular loops of this receptor. This should contribute to further refinement of our understanding of the conformation of this physiologically important receptor and to the molecular basis of its binding its natural peptide ligand.

ACKNOWLEDGMENT

The authors thank Ms. Laura-Ann Bruins for her technical assistance and Dr. Bernard Maigret for sharing the coordinates of his published structure of the CCK-occupied receptor (*11*).

REFERENCES

1. Palczewski, K., Kumasaka, T., Hori, T., Behnke, C. A., Motoshima, H., Fox, B. A., Le Trong, I., Teller, D. C., Okada, T., Stenkamp, R. E., Yamamoto, M., and Miyano, M. (2000) Crystal structure of rhodopsin: A G protein-coupled receptor. *Science 289*, 739–745.
2. Salom, D., Lodowski, D. T., Stenkamp, R. E., Le Trong, I., Golczak, M., Jastrzebska, B., Harris, T., Ballesteros, J. A., and Palczewski, K. (2006) Crystal structure of a photoactivated deprotonated intermediate of rhodopsin. *Proc. Natl. Acad. Sci. U. S. A. 103*, 16123–16128.
3. Cherezov, V., Rosenbaum, D. M., Hanson, M. A., Rasmussen, S. G., Thian, F. S., Kobilka, T. S., Choi, H. J., Kuhn, P., Weis, W. I., Kobilka, B. K., and Stevens, R. C. (2007) High-resolution crystal structure of an engineered human beta2-adrenergic G protein-coupled receptor. *Science 318*, 1258–1265.
4. Rosenbaum, D. M., Cherezov, V., Hanson, M. A., Rasmussen, S. G., Thian, F. S., Kobilka, T. S., Choi, H. J., Yao, X. J., Weis, W. I., Stevens, R. C., and Kobilka, B. K. (2007) GPCR engineering yields high-resolution structural insights into beta2-adrenergic receptor function. *Science 318*, 1266–1273.
5. Ji, T. H., Grossmann, M., and Ji, I. (1998) G protein-coupled receptors. I. Diversity of receptor-ligand interactions. *J. Biol. Chem. 273*, 17299–17302.
6. Schwartz, T. W. (1994) Locating ligand-binding sites in 7TM receptors by protein engineering. *Curr. Opin. Biotechnol. 5*, 434–444.
7. Dufresne, M., Seva, C., and Fourmy, D. (2006) Cholecystokinin and gastrin receptors. *Physiol. Rev. 86*, 805–847.
8. Liddle, R. A. (1997) Cholecystokinin cells. *Annu. Rev. Physiol. 59*, 221–242.
9. Miller, L. J., and Gao, F. (2008) Structural basis of cholecystokinin receptor binding and regulation. *Pharmacol. Ther. 119*, 83–95.
10. Ding, X. Q., Pinon, D. I., Furse, K. E., Lybrand, T. P., and Miller, L. J. (2002) Refinement of the conformation of a critical region of charge-charge interaction between cholecystokinin and its receptor. *Mol. Pharmacol. 61*, 1041–1052.
11. Henin, J., Maigret, B., Tarek, M., Escrieut, C., Fourmy, D., and Chipot, C. (2006) Probing a model of a GPCR/ligand complex in

an explicit membrane environment: the human cholecystokinin-1 receptor. *Biophys. J. 90*, 1232–1240.
12. Hadac, E. M., Pinon, D. I., Ji, Z., Holicky, E. L., Henne, R. M., Lybrand, T. P., and Miller, L. J. (1998) Direct identification of a second distinct site of contact between cholecystokinin and its receptor. *J. Biol. Chem. 273*, 12988–12993.
13. Ji, Z., Hadac, E. M., Henne, R. M., Patel, S. A., Lybrand, T. P., and Miller, L. J. (1997) Direct identification of a distinct site of interaction between the carboxyl-terminal residue of cholecystokinin and the type A cholecystokinin receptor using photoaffinity labeling. *J. Biol. Chem. 272*, 24393–24401.
14. Ding, X. Q., Dolu, V., Hadac, E. M., Holicky, E. L., Pinon, D. I., Lybrand, T. P., and Miller, L. J. (2001) Refinement of the structure of the ligand-occupied cholecystokinin receptor using a photolabile amino-terminal probe. *J. Biol. Chem. 276*, 4236–4244.
15. Gigoux, V., Maigret, B., Escrieut, C., Silvente-Poirot, S., Bouisson, M., Fehrentz, J. A., Moroder, L., Gully, D., Martinez, J., Vaysse, N., and Fourmy, A. D. (1999) Arginine 197 of the cholecystokinin-A receptor binding site interacts with the sulfate of the peptide agonist cholecystokinin. *Protein Sci. 8*, 2347–2354.
16. Kennedy, K., Gigoux, V., Escrieut, C., Maigret, B., Martinez, J., Moroder, L., Frehel, D., Gully, D., Vaysse, N., and Fourmy, D. (1997) Identification of two amino acids of the human cholecystokinin-A receptor that interact with the N-terminal moiety of cholecystokinin. *J. Biol. Chem. 272*, 2920–2926.
17. Escrieut, C., Gigoux, V., Archer, E., Verrier, S., Maigret, B., Behrendt, R., Moroder, L., Bignon, E., Silvente-Poirot, S., Pradayrol, L., and Fourmy, D. (2002) The biologically crucial C terminus of cholecystokinin and the non-peptide agonist SR-146,131 share a common binding site in the human CCK1 receptor. Evidence for a crucial role of Met-121 in the activation process. *J. Biol. Chem. 277*, 7546–7555.
18. Gigoux, V., Escrieut, C., Fehrentz, J. A., Poirot, S., Maigret, B., Moroder, L., Gully, D., Martinez, J., Vaysse, N., and Fourmy, D. (1999) Arginine 336 and asparagine 333 of the human cholecystokinin-A receptor binding site interact with the penultimate aspartic acid and the C-terminal amide of cholecystokinin. *J. Biol. Chem. 274*, 20457–20464.
19. Stryer, L., and Haugland, R. P. (1967) Energy transfer: a spectroscopic ruler. *Proc. Natl. Acad. Sci. U. S. A. 58*, 719–726.
20. Harikumar, K. G., Lam, P. C., Dong, M., Sexton, P. M., Abagyan, R., and Miller, L. J. (2007) Fluorescence resonance energy transfer analysis of secretin docking to its receptor: mapping distances between residues distributed throughout the ligand pharmacophore and distinct receptor residues. *J. Biol. Chem. 282*, 32834–32843.
21. Harikumar, K. G., and Miller, L. J. (2005) Fluorescence resonance energy transfer analysis of the antagonist- and partial agonist-occupied states of the cholecystokinin receptor. *J. Biol. Chem. 280*, 18631–18635.
22. Harikumar, K. G., Pinon, D. I., Wessels, W. S., Dawson, E. S., Lybrand, T. P., Prendergast, F. G., and Miller, L. J. (2004) Measurement of intermolecular distances for the natural agonist Peptide docked at the cholecystokinin receptor expressed in situ using fluorescence resonance energy transfer. *Mol. Pharmacol. 65*, 28–35.
23. Harikumar, K. G., Pinon, D. I., and Miller, L. J. (2006) Fluorescent indicators distributed throughout the pharmacophore of cholecystokinin provide insights into distinct modes of binding and activation of type A and B cholecystokinin receptors. *J. Biol. Chem. 281*, 27072–27080.
24. Ding, X. Q., Dolu, V., Hadac, E. M., Schuetz, M., and Miller, L. J. (2003) Disulfide bond structure and accessibility of cysteines in the ectodomain of the cholecystokinin receptor: specific monoreactive receptor constructs examine charge-sensitivity of loop regions. *Recep. Channels 9*, 83–91.
25. Harikumar, K. G., Pinon, D. I., Wessels, W. S., Prendergast, F. G., and Miller, L. J. (2002) Environment and mobility of a series of fluorescent reporters at the amino terminus of structurally related peptide agonists and antagonists bound to the cholecystokinin receptor. *J. Biol. Chem. 277*, 18552–18560.
26. Haas, E., Katchalski-Katzir, E., and Steinberg, I. Z. (1978) Effect of the orientation of donor and acceptor on the probability of energy transfer involving electronic transitions of mixed polarization. *Biochemistry 17*, 5064–5070.
27. Panchuk-Voloshina, N., Haugland, R. P., Bishop-Stewart, J., Bhalgat, M. K., Millard, P. J., Mao, F., Leung, W. Y., and Haugland, R. P. (1999) Alexa dyes, a series of new fluorescent dyes that yield exceptionally bright, photostable conjugates. *J. Histochem. Cytochem. 47*, 1179–1188.
28. Arlander, S. J., Dong, M., Ding, X. Q., Pinon, D. I., and Miller, L. J. (2004) Key differences in molecular complexes of the cholecystokinin receptor with structurally related peptide agonist, partial agonist, and antagonist. *Mol. Pharmacol. 66*, 545–552.
29. Selvin, P. R. (1995) Fluorescence resonance energy transfer. *Methods Enzymol. 246*, 300–334.
30. Dohlman, H. G., Caron, M. G., DeBlasi, A., Frielle, T., and Lefkowitz, R. J. (1990) Role of extracellular disulfide-bonded cysteines in the ligand binding function of the beta 2-adrenergic receptor. *Biochemistry 29*, 2335–2342.

BI800734W